

Electronic Supplementary Information (ESI) for

**In-situ nitrogen-doped nanoporous carbon nanocables as an
efficient metal-free catalyst for oxygen reduction reaction**

Wen-Jie Jiang,^{a,b} Jin-Song Hu,^{*a} Xing Zhang,^a Yan Jiang,^a Bin-Bin Yu,^a Zi-Dong Wei,^{*b} and Li-Jun Wan^{*a}

^a Beijing National Laboratory for Molecular Sciences, Key Laboratory of Molecular Nanostructure and Nanotechnology, Institute of Chemistry, Chinese Academy of Science, 2 North 1st Street, Zhongguancun, Beijing 100190, China.

^b State Key Laboratory of Power Transmission Equipment & System Security and New Technology, College of Chemistry and Chemical Engineering, Chongqing University, Chongqing 400044, China.

E-mail: hujs@iccas.ac.cn, zdwei@cqu.edu.cn, wanlijun@iccas.ac.cn,

This Electronic Supplementary Material includes:

Supplementary Figures S1-S4, Table S1-S2

Supplementary References

Fig. S1. SEM image (a), TEM image (b) and High-resolution TEM image (c) of CNT@NPC-800. SEM image (d), TEM image (e) and High-resolution TEM image (f) of CNT@NPC-1000.

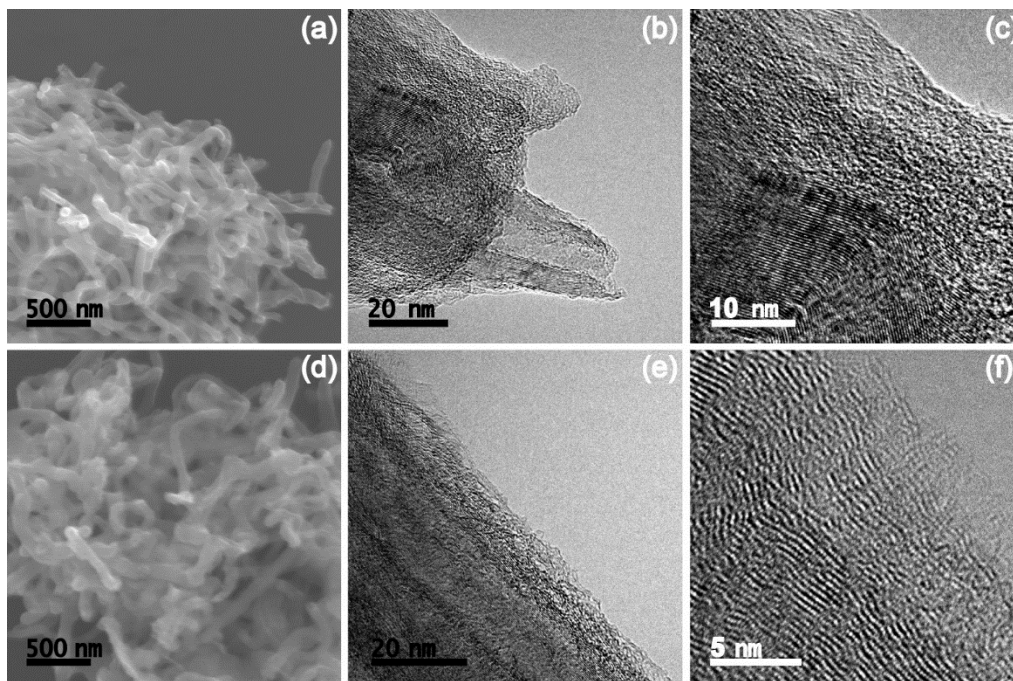


Fig. S2. Typical TEM image of CNT@NPC obtained after hydrothermal synthesis but before pyrolysis. The exposed CNT tips marked in orange circles could enhance the role of three-dimensional conductive network of CNTs in catalysts and facilitate the electron migration.

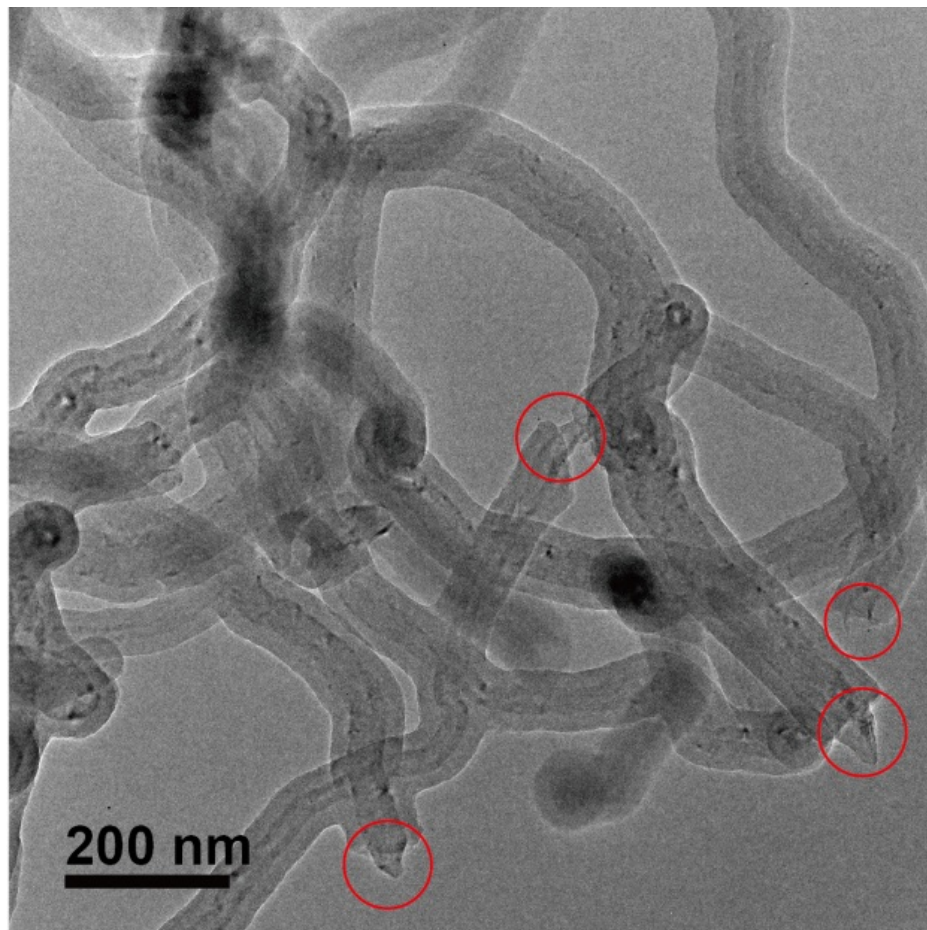


Fig. S3. N₂ adsorption-desorption isotherms of acid purified CNTs (a), CNT@NPC-800 (c), and CNT@NPC-1000 (e). Pore size distribution of CNTs (b), CNT@NPC-800 (d), and CNT@NPC-1000 (f) from analysis of the desorption branch using the Barrett-Joyner-Halenda (BJH) method.

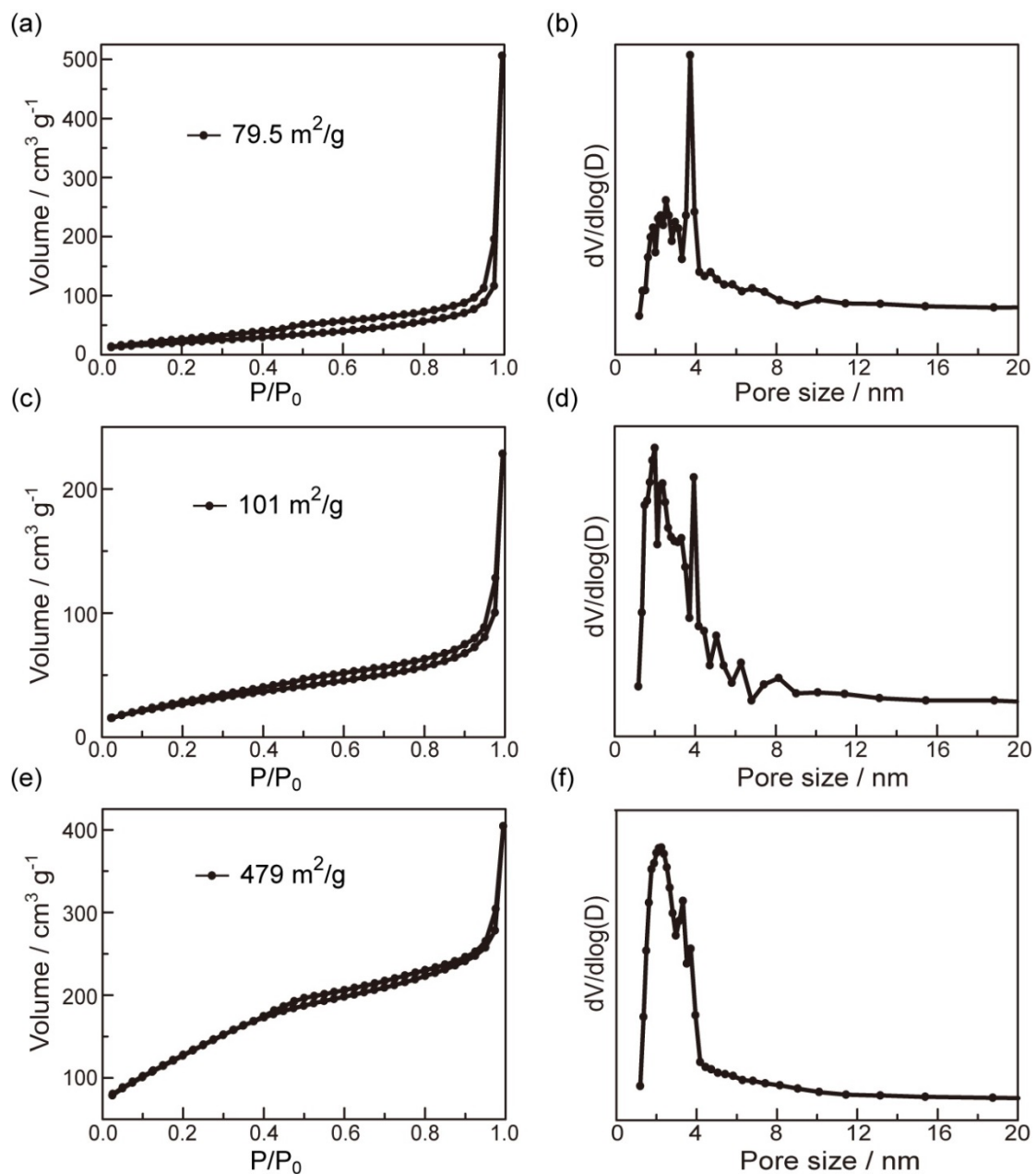


Fig. S4. LSV curves recorded in O₂-saturated 0.1 M KOH solution at various rotating speeds for CNT@NPC-800 (a), CNT@NPC-900 (c), CNT@NPC-1000 (e), and commercial Pt/C (g). Koutecky-Levich plots at various potentials for CNT@NPC-800 (b), CNT@NPC-900 (d), CNT@NPC-1000 (f), and commercial Pt/C (h).

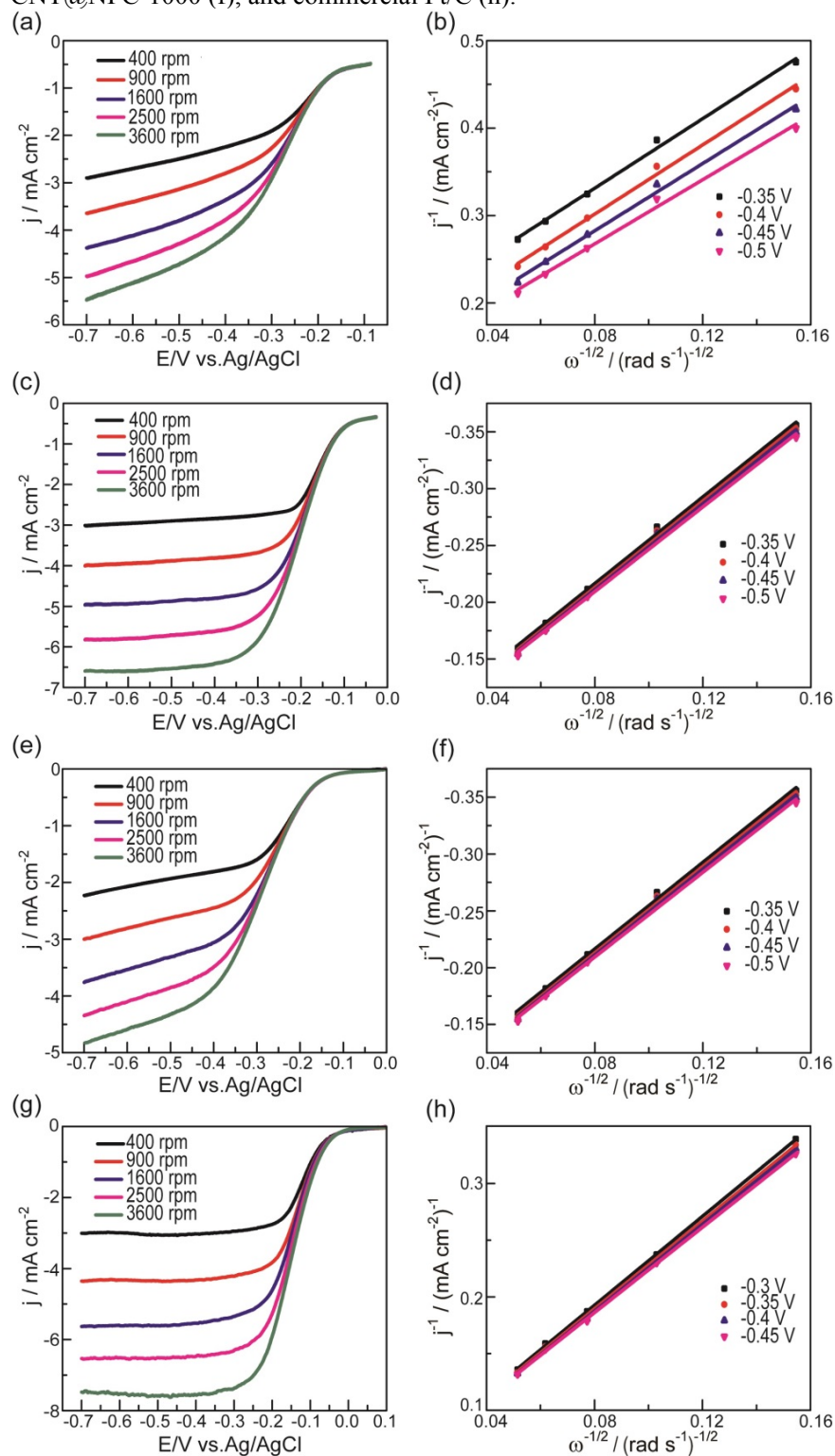


Table S1. Binding energy position of pyridinic type, pyrrolic type, and quaternary type nitrogen used in the deconvolution of the XPS N1s peaks of CNT@NPCs shown in Fig. 2. [S2]

	pyridinic-N (eV)	pyrrolic-N (eV)	quaternary-N (eV)
CNT@NPC-800	398.32	399.51	400.72
CNT@NPC-900	398.07	398.93	400.83
CNT@NPC-1000	398.51		400.97

Table S2. Comparison of electrocatalytic activity of CNT@NPC-900 with other metal-free carbon materials previously reported in literatures measured in 0.1 M KOH solution. The potential is versus Ag/AgCl unless specifically noted.

Catalysts	Onset potential (V)	Cathodic ORR peak (V)	Half-wave potential (V)	Mass current density ^[a] (mA/mg)	References
CNT@NPC-900	-0.114	-0.253	-0.184	8.43 at -0.2 V 38.5 at -0.2 V	this work
Commercial JM Pt/C	-	-	-0.142	11.9 at -0.1 V	this work
N-doped graphene dots	-0.16	-0.27	-0.363	~1.5	<i>J. Am. Chem. Soc.</i> 2012 , 134, 15
Polyelectrolyte-functionalized graphene	-0.15	-0.35	-0.372	-	<i>ACS Nano</i> 2011 , 5, 6202
Polyaniline-derived N- and O-doped mesoporous carbons	-0.095	-0.553	-0.342	~0.94	<i>J. Am. Chem. Soc.</i> 2013 , 135, 7823
Edge-halogenated graphene nanoplatelets	-0.14	-0.22	-0.345	~4.67	<i>Sci. Rep.</i> 2013 , 3, 1810
Vertically aligned BCN nanotubes	-0.009	-0.295	-0.219	-	<i>Angew. Chem. Int. Ed.</i> 2011 , 50, 11756
BCN graphene	-0.055	-0.323	-0.245	-	<i>Angew. Chem. Int. Ed.</i> 2012 , 51, 4209
N-doped carbon sub-micrometer spheres	-0.1	-0.218	-0.247	2.5 at -0.2 V	<i>Adv. Mater.</i> 2013 , 7, 998
Sulfur and nitrogen doped carbon aerogels	-0.13	-0.341	-0.289	1.14 at -0.2 V	<i>Green Chem.</i> 2012 , 14, 1515

[a] The data in this column may be influenced by the difference in system configuration. The value is obtained from measured current density divided by catalysts loading.

Supplementary reference:

- [S1] S. Wang, D. Yu, L. Dai, D. W. Chang, J.-B. Baek, *ACS Nano* **2011**, *5*, 6202-6209.
- [S2] L. Lai, J. R. Potts, D. Zhan, L. Wang, C. K. Poh, C. Tang, H. Gong, Z. Shen, J. Lin, R. S. Ruoff, *Energy Environ. Sci.* **2012**, *5*, 7936-7942